Journal of Nanostructure in Chemistry (2021) 11:455–468
https://doi.org/10.1007/s40097-020-00380-8

ORIGINAL RESEARCH

Functional Co_3O_4 nanostructure-based electrochemical sensor for direct determination of ascorbic acid in pharmaceutical samples

Nadir H. Khand[1] · Ismail M. Palabiyik[2] · Jamil A. Buledi[1] · Sidra Ameen[1,3] · Almas F. Memon[1] · Tania Ghumro[1] · Amber R. Solangi[1]

Received: 23 August 2020 / Accepted: 15 December 2020 / Published online: 4 January 2021

Abstract

Ionic liquid (IL)-assisted Co_3O_4 nanostructures were synthesized by a simple, facile and novel low-temperature aqueous chemical growth method and used for the modification of glassy carbon electrode (GCE) for the selective determination of ascorbic acid (AA). Different volumes of IL were used in the preparation of nanostructures to examine the effect of IL on the morphology and electrochemical performance of the synthesized material. The functionalities of the prepared material were investigated by FTIR, while the crystalline nature and phase purity of the material were confirmed by XRD results. FESEM analysis were carried out to expose the surface characteristics of the prepared nanostructures and the results demonstrated that the cobalt oxide nanostructures possess nanorods like morphology. The EDX results verified the maximum elemental percent composition for the cobalt and oxygen in the synthesized material. The electrochemical performance of Co_3O_4 nanostructures modified GCE was investigated by cyclic voltammetry (CV) and electrochemical impedance spectroscopy (EIS). The electrochemical results demonstrated that the modified electrode shown outstanding performance in the determination of AA with a very low limit of detection (1 μM) along with higher stability and repeatability features. The novel AA sensor manifested exceptional sensitivity and selectivity over a wide linear range of concentration from 0.05 to 3 mM with the coefficient of determination $R^2 = 0.998$. The applicability of the developed sensor was examined in the pharmaceutical samples that contain AA and the sensor selectively detected the AA from multiple ingredients that were present in their formulation with acceptable recovery.

✉ Amber R. Solangi
ambersolangi@gmail.com; amber.solangi@usindh.edu.pk

[1] National Centre of Excellence in Analytical Chemistry, University of Sindh, Jamshoro 76080, Pakistan

[2] Department of Analytical Chemistry, Faculty of Pharmacy, Ankara University, Ankara, Turkey

[3] Department of Chemistry, Shaheed Benazir Bhutto University, Shaheed Benazirabad, Sindh 67450, Pakistan

Graphic abstract

It describes the synthesis of [BMIM][PF_6] IL functionalized cobalt oxide nanostructures through low-temperature aqueous chemical growth method and the synthesized material was utilized to fabricate an electrochemical sensor (Co_3O_4/GCE) for the selective determination of Ascorbic acid.

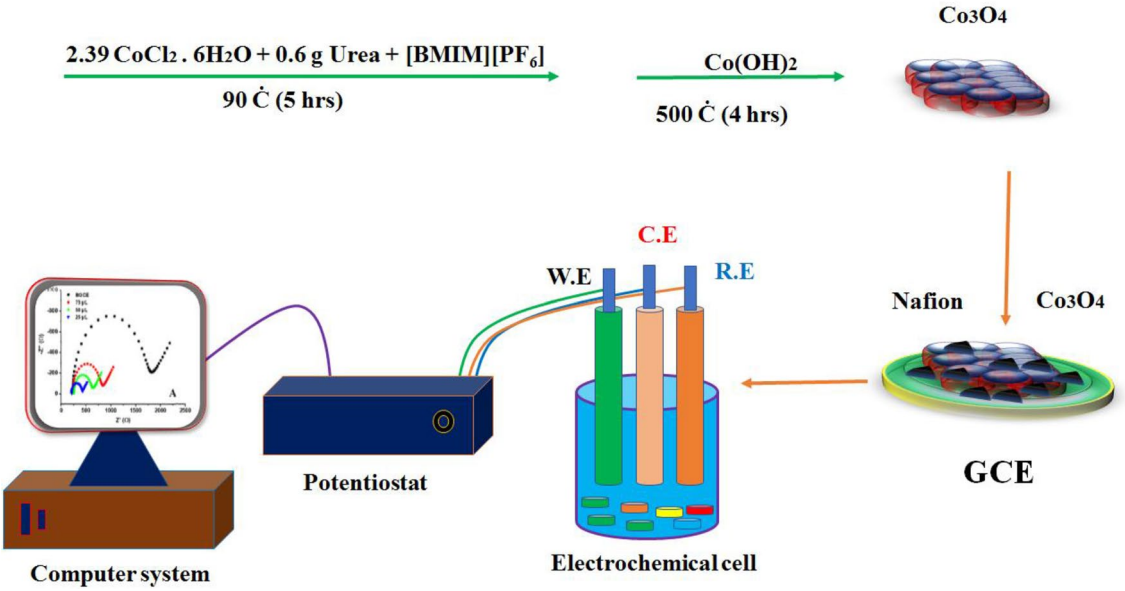

Keywords Co_3O_4 nanostructures · Ionic liquid-assisted synthesis · Electrochemical sensor · Ascorbic acid · Vitamin C

Introduction

Ascorbic acid (AA) is an essential water-soluble vitamin, which is present naturally in fruits (lemon, orange, tomato and pepper), leafy vegetables and drinks. It is commonly known as vitamin C [1]. AA is widely used in food processing, pharmaceutical formulations, animal feed, multivitamin tablets and in the cosmetic application as an antioxidant [2, 3]. The dehydroascorbic acid or ascorbic acid is the oxidized form of hexuronic acid [4]. AA is necessary to the human diet because it possesses an important role in metabolisms and helps in scavenging free radicals [3, 5], improving immunity and promoting cell development [6]. AA also plays a vital role in the treatment of psychological illness, prevention from cancer disease [7], infertility and Acquired Immune Deficiency Syndrome (AIDS) [8]. It also helps in healing burns or injuries, forming blood vessels, scar tissues, etc. The deficiency of AA can cause severe diseases commonly called scurvy and cataracts [9]. Scurvy has some symptoms such as tiredness, joint pain, muscle rashes or weakness, etc. [10]. Owing to the fundamental role of AA in human life as well as in industries, it is important to develop a rapid method by which selective, fast, accurate and sensitive determination of AA could be possible.

There are many reported methods for the detection of AA including high-performance liquid chromatography [11], colorimetric methods [12], capillary electrophoreses [13], chemiluminescence [14], spectrophotometry [15], fluorometry [16] and enzymatic analysis [17]. However, these traditional methods are very costly, time-taking and not applicable for routine applications. Especially, the HPLC or CE methods require complex sample handling, large instruments, trained technicians as well as expensive reagents which may not be readily available [18–20]. There is a strong need to develop a highly sensitive and selective method that must be simple and suitable for onsite detection of AA.

Electrochemical techniques have gained great attention for the quantitative detection of AA because of its high sensitivity and selectivity, easy process and low-cost features [21–23]. Conversely, during the electrooxidation of AA and consequent adsorption of dehydroascorbic acid on the bare carbon-based electrode surface (glassy carbon and graphite), the overvoltage is usually high which results in fouling of electrode, low sensitivity, poor selectivity and reproducibility [24]. To deal with these limitations, nanomaterials are extensively used as electrocatalysts to modify the electrodes and to increase the analytical performance of electrochemical sensors [25, 26]. Nowadays, a variety of nanomaterials

are being used for the modification of electrodes including noble metals [20], polymers [27], metal oxides [28–30], carbon materials [31, 32] and quantum dots [24]. Among these nanomaterials, metal oxides have attracted much attention because of their high surface area, excellent working ability, better synthetic accessibility, wide band gapes and good catalytic performance [33–36]. From metal oxides, NiO, CuO, TiO_2, MnO_2, or ZnO nanostructures are used along with other electroactive materials such as graphene CNT or conducting polymers to enhance their stability and electrochemical behavior [37–39]. Amongst these metal oxides, Co_3O_4 nanostructures have attracted scientist's attention due to their best electrocatalytic activity, enhanced surface area and low-cost features [40, 41]. It is a p-type ferromagnetic semiconducting transition metal oxide that has band gaps of 2.10 eV and 1.60 eV correspondingly. In the Co_3O_4 compound, Co^{2+} and Co^{3+} ion pairs coexist at the same time in which Co^{3+} ions occupy octahedral sites and Co^{2+} ions occupy tetrahedral sites with oxygen ions and forming a closely packed face-centered cubic lattice. It crystallizes in spinal structure and this type of arrangement of ions ensures that Co_3O_4 has explicit surface topographies with different polar terminations [42]. Co_3O_4 NPs possess some outstanding properties such as optical, electrical, electrochemical and electrocatalytic, therefore, used in a large number of potential applications in electrochemical sensors [43] supercapacitor [44], Li-ion batteries [45], etc.

Ionic liquids (ILs) are the class of low-temperature organic molten salts and possess a wide range of temperatures. ILs can be used in catalysis [46], as an inert solvent in electrochemistry [47] and in some chemical process, it can be used to replace water due to their unique properties such as high polarity, negligible vapor pressure, good dissolving ability, tailorable structures, high thermal stability and high ionic conductivity [48]. ILs have been used as solvents, morphological templates, additives and reactants for the synthesis of inorganic nanomaterial with excellent properties [49, 50]. An important feature of using ILs in the synthesis of nanostructures involves the growth and nucleation of nanoparticles [51]. The main focus of the present study while utilizing IL for the synthesis of cobalt oxide nanostructures is to effectively control the size, shape, morphology, stability and to enhance the electrocatalytic efficiencies of prepared Co_3O_4 nanostructures for the fluent determination of AA. In this study, [BMIM][PF_6^-] IL was utilized as a morphological template, which composed of 1-butyle-3-methylimidazolium cations and hexafluorophosphate anions. The cationic part of the ionic liquid has high electron-accepting capabilities due to the delocalized aromatic system that causes electrostatic attraction with polar moieties of the material and interact via π-interaction. Moreover, the single hydrogen atom linked with the C-2 carbon atom of the imidazolium ring possesses an acid character that may form hydrogen bonds with oxygen or hydroxide atoms of the nanomaterial. It is reported that the hydrogen-bond-cobalt-π-π-stack mechanism is responsible for the formation of a synthesized nanostructure framework [52]. The possible functionalization mechanism of Co_3O_4 nanostructures by [BMIM][PF_6^-] IL is given in Scheme 1.

To the best of our knowledge, based on the available literature, we can say that there is no report before on using just Co_3O_4 nanostructures for the selective electrochemical sensing of AA. However, extensive work has been carried out on using different nanomaterials for the determination of AA that reports lower LOD and wider linear range, but most of the reported works are based on composite materials, graphene-based [24] or polymer-based nanomaterials that are formed by utilizing expensive and toxic chemicals which are hazardous for the environment as well.

Herein, in this work, we report the synthesis of Co_3O_4 nanostructures with the assistance of ionic liquid through the aqueous chemical growth method which is almost a greener method for the environment and generally requires water as a reaction medium and also performed at a very

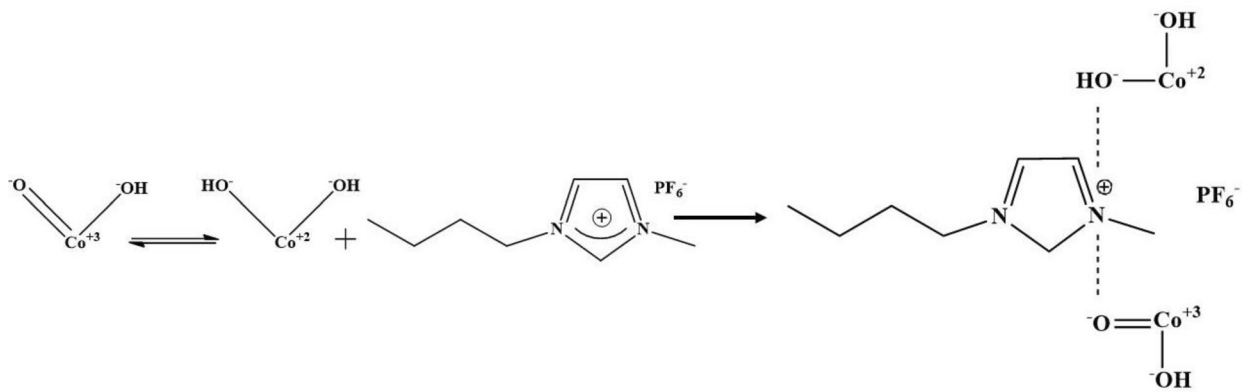

Scheme 1 The possible functionalization mechanism of Co_3O_4 nanostructures by [BMIM][PF_6^-] IL

low temperature. The synthesized nanostructures were utilized to fabricate an electrochemical sensor for the selective detection of AA. Due to the prodigious catalytic activity, large surface area and highly conductive nature of Co_3O_4 nanostructures, the proposed Co_3O_4/GCE sensor has shown outstanding performance for the detection of AA in chemical as well as in real pharmaceutical samples. The overall obtained results are good and comparable with the previously reported work.

Experimental

Reagent and solutions

AA, cobalt chloride hexahydrate and urea were purchased from Sigma-Aldrich (UK and Sweden). 1-butyl-3-methyl imidazolium hexafluorophosphate $[BMIM]^+[PF_6]^-$ IL was purchased from Fluka (Switzerland). All the chemicals were of analytical grade and used without any further pretreatment. The phosphate buffer solution (PBS) of 0.1 M concentration was prepared in deionized (D.I) water which was used as a supporting electrolyte throughout the experiment. The pH of the solution was maintained at 7.4 by adjusting it with 0.1 M NaOH and HCl. The glassware was washed with tap water and rinsed several times with D.I. water.

Synthesis of Co_3O_4 nanostructures

The synthesis of Co_3O_4 nanostructures was done through aqueous chemical growth method. It is a simple, prolific, rapid and low-temperature approach. The main advantage of this method is the use of water as the solvent. In this regard, three separate solutions containing 0.1 M metal salt ($Co\ Cl_2.6H_2O$) and 0.1 M urea were prepared in 100 mL of D.I. water followed by the addition of variant volumes (25, 50 and 75 µLs) of IL $[BMIM]^+[PF_6]^-$ in each solution. The amount of precursor salt and urea were kept constant in all solutions, only the volume of IL was varied. The beakers containing the chemical mixture were kept on magnetic stirring for several minutes to homogenize the mixture. After that, the beakers were fully wrapped with aluminum foil and placed in a heating oven for 5 h at 90 °C for the growth of nanostructures. As the time was completed, the formed cobalt hydroxide precipitates were filtered through Whatman filter paper and washed many times with D.I water to remove the rest of the impurities. The filtered material was then dried in an oven for 30 min at about 80 °C and annealed in an electric furnace at 500 °C for 4 h to convert cobalt hydroxide nanostructures into pure Co_3O_4 nanostructures.

Modification of GCE

The GCE electrode was modified by the drop-casting method and the solution was prepared as reported in the literature [53]. For the modification of GCE, 10 mg of Co_3O_4 nanostructure powder and 50 µL of Nafion 5% was added in 2.5 mL D.I. water and the solution was sonicated for 15 min. Before the modification, the electrode surface was thoroughly cleaned by polishing with 0.5 µm pore alumina powder and washed with D.I. water. After that, the modification was done by dropping 10 µL of prepared Co_3O_4 nanostructures solution carefully on the surface of the electrode and the electrode was left for drying at room temperature. The same procedure of modification was followed for all three prepared materials.

Instrumentation and electrochemical parameters

The functional group analysis of the prepared Co_3O_4 nanostructures was evaluated by using Fourier-transform infrared spectrophotometer (Thermo Nicolet 5700), the crystalline nature and the phase recognition of Co_3O_4 nanostructures were done through X-ray powder diffraction (XRD) using Phillips PW 1729 powder diffractometer and the conformation of the elemental composition of the materials was carried out by energy-dispersive spectroscopy (EDS). While the shape and surface morphological characteristic of the synthesized material was assessed by field emission scanning electron microscopy (FESEM) by using LEO 1550 Gemini worked at 20 kV. Whereas, all the electrochemical experiments were performed on CHI 760D electrochemical workstation (USA). A proper three-electrodes containing conventional assembly was established in which Co_3O_4 NPs modified GCE or Co_3O_4NPs/GCE utilized as working electrode along with counter electrode (platinum wire) and a reference electrode (Ag/AgCl), respectively. The CV studies were carried out in the potential range of -0.8 to $+0.8$ V at the scan rate of 60 mV s^{-1} in 0.1 M PBS of 7.4 pH. The CV current response of AA appeared at $+0.2$ V vs. Ag/AgCl electrode. All the experimental measurements were performed at room temperature.

Real sample preparation

To explore the practical applicability of the proposed sensor, three different pharmaceutical samples namely "Calci, CaC 1000 + and Surbex Z" were purchased from local medical stores of Jamshoro city, Sindh, Pakistan. For the preparation of the real sample solution, initially, three tablets of CaC 1000 + were crushed in a mortar and powdered. The powder was then dissolved in 100 mL of D.I. water followed by the sonication for 30 min. After the sonication process, the solution was filtered twice by Whatman 42 filter paper to remove

the impurities and get a transparent solution and then it was used for further investigations by diluting an appropriate amount of filtered solution into an electrolyte solution and the measurements were carried out using CV technique to investigate the applicability of the fabricated Co_3O_4/GCE in real samples followed by calibration method. The same procedure was followed for the preparation and analysis of two other (Calci and Surbex Z) pharmaceutical samples.

Results and discussion

Characterization of Co_3O_4 nanostructures

To evaluate different functionalities present in cobalt oxide nanostructures synthesized with different volumes of ionic liquids, the FTIR study was carried out. The wavelength of IR was set from 400 to 2750 cm^{-1}. The two IR bands that appeared at 497.5 and 640.2 are the characteristic vibration modes of (Co–O) which confirm the successful fabrication of spinal cobalt oxide nanostructures. While the IR band appeared at 1643.1 is OH bending vibration of H_2O absorbed from the atmosphere. The IR bands of cobalt oxide nanostructures synthesized with 25, 50 and 75 µL of IL are displayed in Fig. 1. From the IR spectrum, no visible difference was observed except the intensities of IR characteristic peaks.

The crystallinity and the phase transparency of the material were inspected through powder X-ray diffraction (XRD) and the obtained results of Co_3O_4 nanostructures prepared with different volumes of IL are shown in Fig. 2a. The peaks located at 2θ represent the crystal planes of (111), (220), (311), (222), (400), (511) and (440) spinal cubic phase of Co_3O_4 and are identical with standard JCPDS card No: 43-10003. The sharpness of the peaks indicates the high crystalline nature of the synthesized nanostructures, while the absence of other phase peaks demonstrates the purity of the prepared material. The average crystalline size of the prepared materials was calculated from the major XRD diffraction peaks by using the Scherer equation ($\tau = k\lambda/(\beta \cos\theta)$) and it was observed to be 22.9 nm for the material in which 25 µL volume of IL was added and 24.7 nm and 27.5 nm for the materials in which 50 and 75 µL volumes of IL were added, respectively. Furthermore, to ensure the elemental composition of the as-prepared materials, EDX (energy-dispersive spectroscopy) analysis was carried out and the results confirmed only the presence of Co and O elements in the fabricated material as given in Fig. 2b. The total weight percentage of cobalt and oxygen elements were found 67.7% and 31.4% in the material that was prepared with 25 µL of IL; and 67.9%, 31.3% for the material which contains 50 µL of IL and 69.8%, 31.1% for the material which was synthesized with 75 µL of IL, respectively.

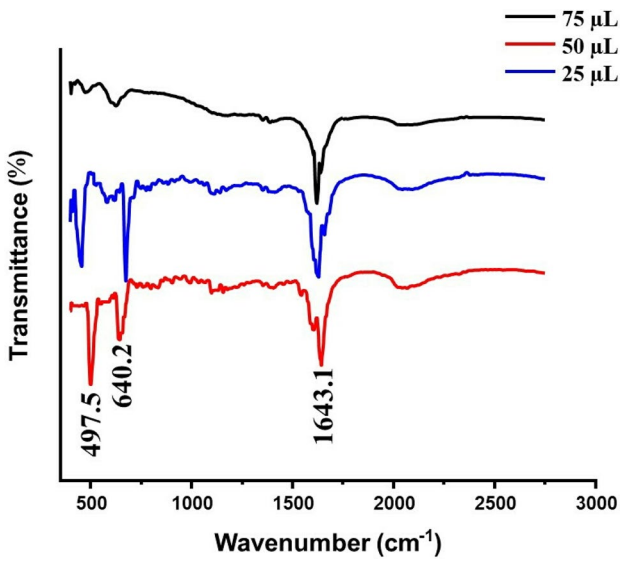

Fig. 1 FTIR spectrum of Co_3O_4 nanostructures prepared using different volumes of IL (blue) 25 µL, (red) 50 µL, and (black) 75 µL

The structural characteristics or shape of the prepared Co_3O_4 nanostructures and the effect of IL on the morphology of prepared Co_3O_4 nanostructures were studied through FESEM analysis. Figure 3a–f contains different high- and low-resolution images of the materials in which different volumes of IL have been used. In Fig. 2a, b are the images of that material in which 25 µL of IL were utilized while c, d and e, f are the images of the materials in which 50 and 75 µLs of IL were added, respectively. These images are showing that the prepared material is in nano-rod-like shape and all three materials are showing almost identical shape which indicates that the higher volumes of IL did not significantly affect the shape of the prepared material.

Electrochemical characterization of bare and modified electrodes

Electrochemical characterization was carried out using EIS and CV technique in 5 mM $[Fe(CN)_6]^{-3/-4}$ and 0.1 M KCl solution used as redox probe to manifest the interfacial characteristics of bare and modified electrodes. EIS is a powerful method to investigate the electron transfer ability or electron transfer resistance (*R*ct) properties of various chemically modified electrodes. In EIS, the semicircle part in the high-frequency region corresponds to the electron transfer activity and the diameter of that semicircle is directly proportional to the *R*ct value of different electrodes, meanwhile, in the low-frequency region, the linear part corresponds to the diffusion process [54, 55]. The *R*ct value of bare and different modified electrodes was obtained through fitting Randles equivalent electric circuit diagram: *R*s CPE(*R*ct-*Z*w) and the resultant Nyquist plot of bare and different Co_3O_4 modified

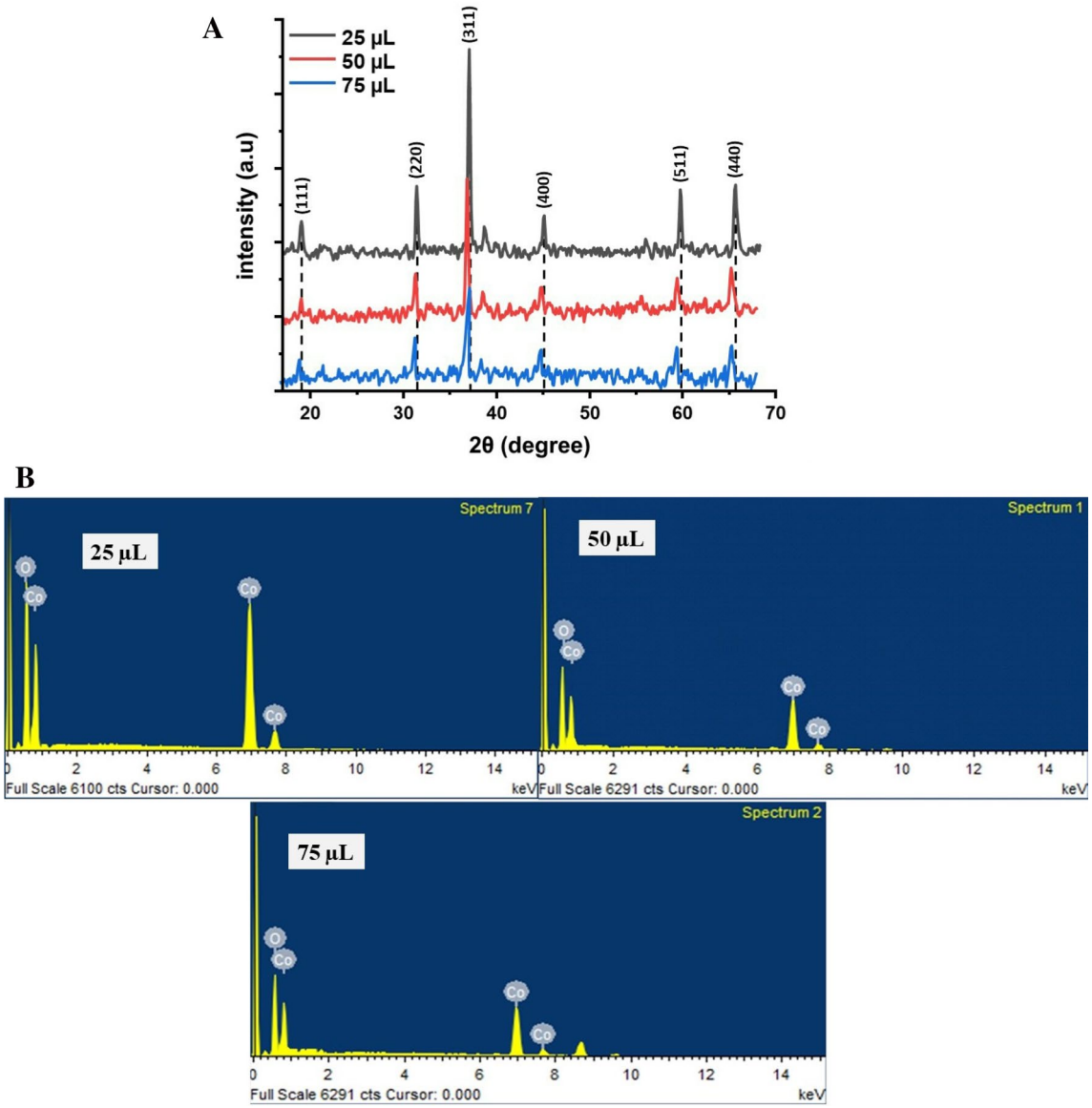

Fig. 2 **a** XRD patterns of Co_3O_4 nanostructures synthesized with 25 µL (black), 50 µL (red) and 75 µL (blue) volumes of IL. **b** Shows the EDX results of synthesized nanostructures prepared with variant amounts of IL

GCEs is shown in Fig. 4a. The largest semicircle diameter and highest *R*ct value were obtained at bare GCE (1475 Ω) indicating that bare GCE has less conductivity and very poor electron transfer efficiency. However, with different Co_3O_4 modified electrodes, the smallest semicircle diameter and lowest *R*ct value (202.7 Ω) was obtained with the material in which 25 µL of IL was utilized, indicating that this material has high electron transferring efficiency and providing more active surface area which might be due to the small size of the particles as compared to the other two materials that have the *R*ct values of 356 Ω and 568.4 Ω (for 50 and 75 µL IL), respectively. The active surface area of bare and modified electrodes was determined by Randles–Ševčík equation: "$I_p(\mu A) = 2.69 \times 10^5 \times n^{3/2}\, AD^{1/2}\, \upsilon^{1/2}\, C$". The active surface area for bare GCE was observed to be 6.12 mm^2, while for the modified electrodes, it was calculated to be 9.76, 8.45 and 7.24 mm^2 for the materials in which 25, 50 and 75 µLs of IL were used.

Figure 4b displays the CV response of various Co_3O_4 modified GCEs and bare GCE obtained in 5 mM $[Fe(CN)_6]^{-3/-4}$ and 0.1 M KCl redox probe solution. As can be seen from the voltammogram, that as compared to the bare GCE and other two Co_3O_4 modified GCEs (in which 50, 75 µL of IL were used) a well-resolved peak with high redox peak current was obtained from Co_3O_4 prepared with 25 µL volume of IL.

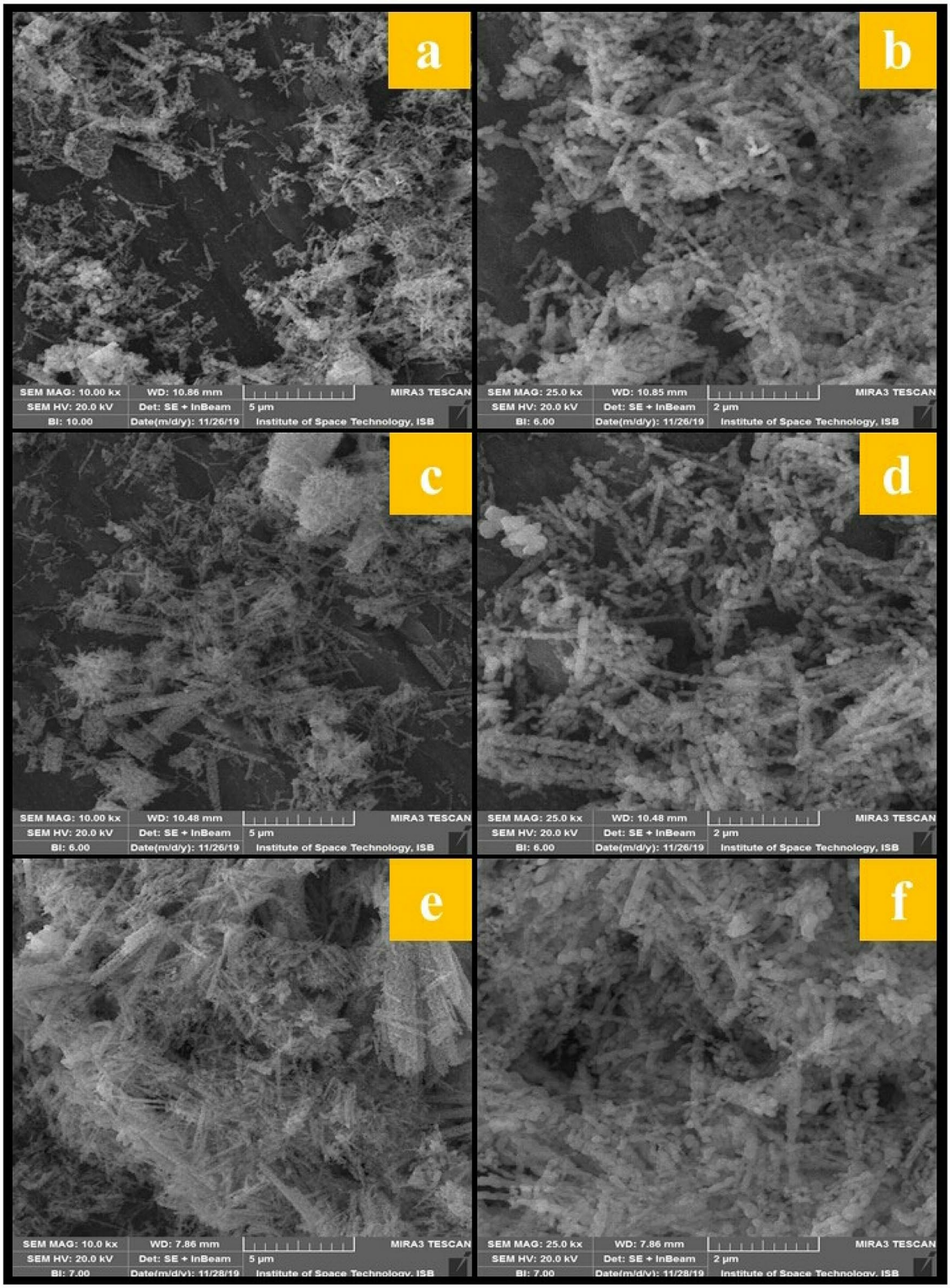

Fig. 3 Low- and high-resolution FESEM images of Co_3O_4 nanostructures that were prepared with 25 µL (**a**, **b**), 50 µL (**c**, **d**) and 75 µL (**e**, **f**) volumes of IL

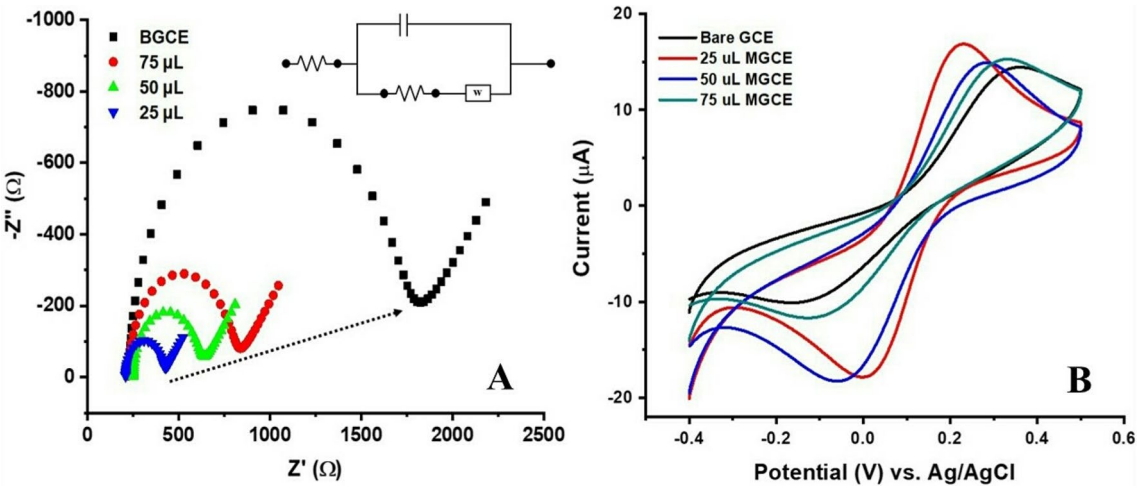

Fig. 4 **a** Nyquist plot, **b** CV curves of bare and different Co_3O_4 modified GCEs recorded in 5 mM $[Fe(CN)_6]^{-3/-4}$ and 0.1 M KCl solution

Electrochemical behavior of AA on bare and different modified electrodes

To check the electrochemical response of the Co_3O_4/GCE sensor towards the oxidation of AA, the CV technique was used. Figure 5a shows the cyclic voltammogram of bare and modified GCE in the presence and absence of 0.1 mM AA in 0.1 M PBS of pH 7.4. As can be seen from the voltammogram that in the absence of AA, both modified and bare GCEs exhibited no response which means that no redox activity was taken place on the electrode surfaces. Meanwhile, as compared to the bare GCE, a high oxidation peak current at about + 0.2 V was observed with modified Co_3O_4/GCE in the presence of AA, indicating the fast electron transfer rate on the modified electrode surface. It can also be noticed that the potential also shifted towards the less positive value on modified electrode response which reveals the less over potential as compared to the bare electrode. The electrochemical oxidation reaction of AA involved two-electron and two proton process. The possible oxidation reaction mechanism AA is illustrated in Scheme 2.

Figure 5b displays the CV response voltammogram of different Co_3O_4/GCEs towards AA oxidation. The figure shows that, amongst the Co_3O_4 nanostructures prepared with variant volumes of IL, the nanostructures prepared with 25 µL of IL have shown slightly higher oxidation current and a sharp peak as compared to the other two nanostructures (which have shown slightly lower oxidation current response) that might be due to the small size of the nanostructures that were prepared with 25 µL of IL. The variation in the size of

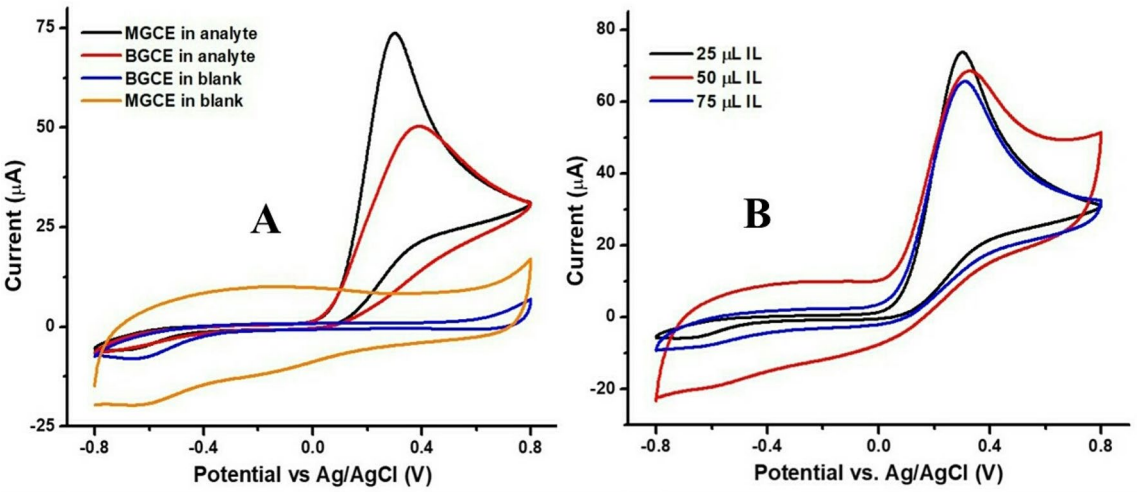

Fig. 5 **a** CV response of Co_3O_4/GCE (black and orange line) and bare GCE (red and blue line) in presence and absence of 0.1 mM AA in 0.1 M PBS of pH 7.4 **b** CV response of different Co_3O_4/GCEs recorded in presence of 1 mM AA

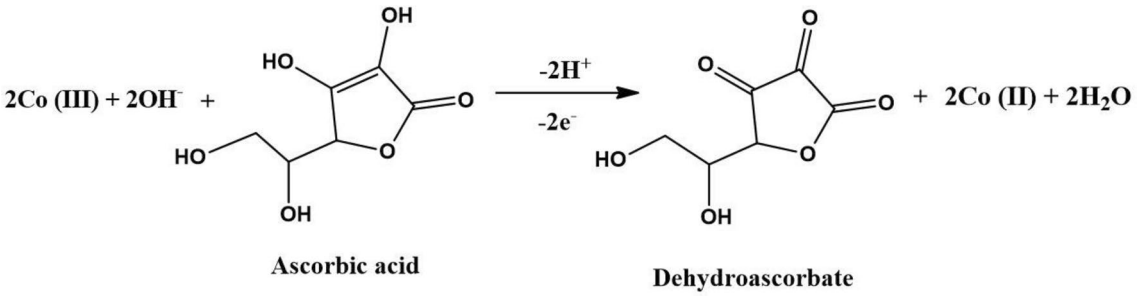

Scheme 2 The possible oxidation reaction mechanism of AA at Co_3O_4/GCE sensor

the nanostructures by varying the volumes of IL is leading to the fact that ILs are well known for their high stabilizing characteristic and used in the synthesis of nanomaterials for the nucleation and growth of nanoparticles. By increasing the volume of IL, the size of the particles decreased very much and because of their magnetic property, they agglomerated quickly which influence the overall performance and catalytic efficiency of the Co_3O_4 nanostructures. We have taken several runs of each modified electrode to ensure the stability and good catalytic ability of individual material toward AA oxidation and every time the mentioned material shown the best results. Thus, all the other parameters were optimized on this material.

Effect of supporting electrolyte and pH

To check the effect of electrolytes on AA oxidation peak current, different buffer solutions were used as supporting electrolytes such as borate buffer (pH-10), NaOH (pH-12) and phosphate buffer (pH 7.4). Figure 6a displays the CV response of AA oxidation in these electrolytic solutions. As can be seen from the Figure that a sharp and well-resolved peak has appeared in the phosphate buffer as compared to the NaOH and borate buffers. Therefore, the phosphate buffer was chosen as a supporting electrolyte for the sensitive determination of AA. Moreover, the pH of the supporting electrolyte has also a great influence on the oxidation response of AA. Thus, the fabricated electrode was tested in 0.1 M PBS of various pH ranges from 5–8 in the presence of 1 mM AA. As, it can be seen from Fig. 6b that the oxidation peak current of AA has a high dependency on pH. As the pH of the supporting electrolyte increases, the oxidation peak current of AA has also increased and reached the maximum at a pH of 7.4 and then, a sudden decrease can be seen in the peak current when pH increased to 8. Meanwhile, the peak potential of AA oxidation can also be observed to slightly shift negatively with the increased pH which indicates that proton involving reaction is taking place at Co_3O_4/GCE surface.

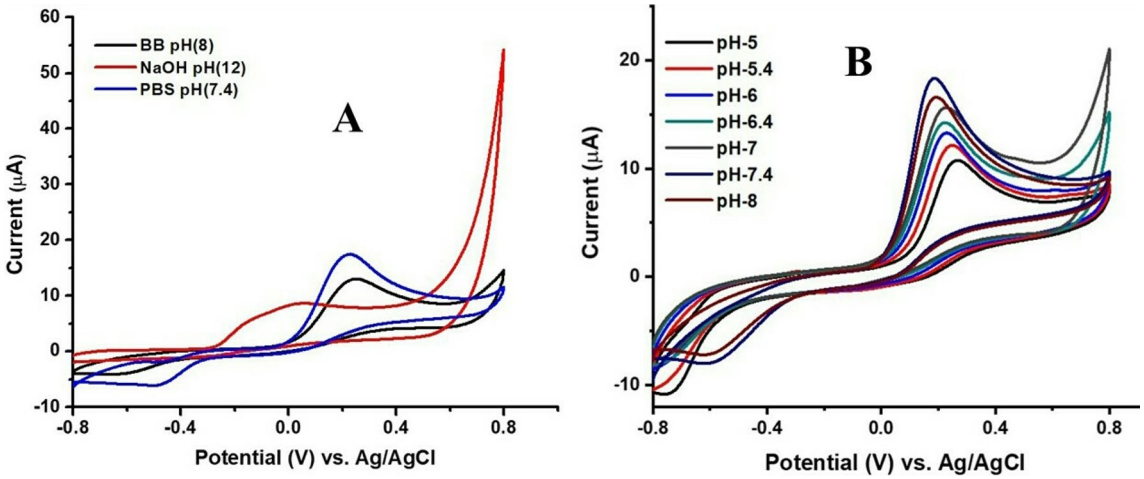

Fig. 6 **a** Effect of different supporting electrolytes of various pH values on Ipa of 1 mM AA, **b** CV response of Co_3O_4/GCE against 0.1 mM AA in 0.1 M PBS of different pH ranges from 5–8

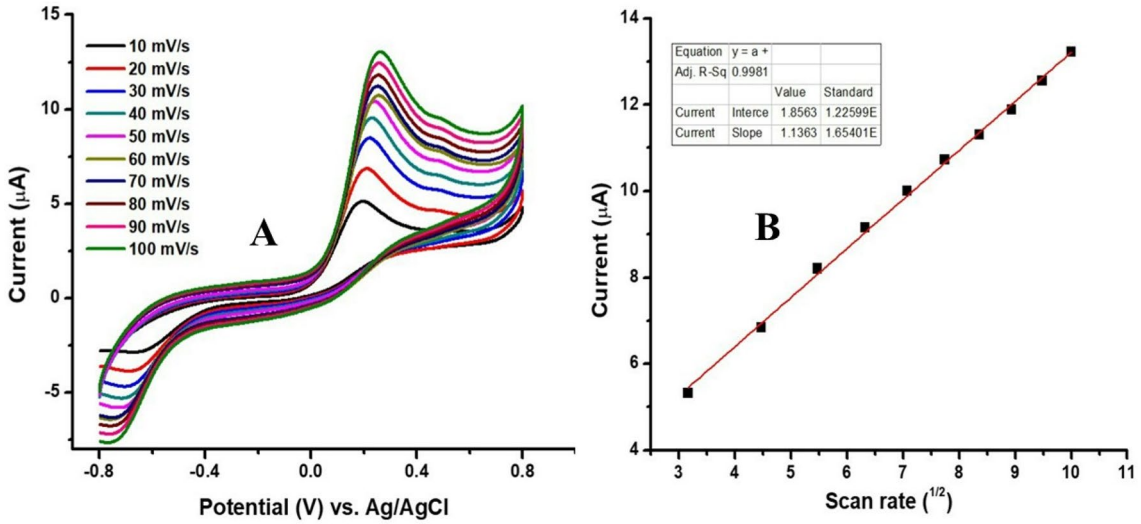

Fig. 7 **a** CV response of Co_3O_4/GCE against 0.1 mM AA in 0.1 M PBS (pH 7.4) at different scan rates from 10 to 100 mVs^{-1}. **b** The linear correlation plot of oxidation peak current vs. square root of scan rate with $R^2 = 0.998$

Effect of scan rate

The effect of scan rate (from 10 to 100 mV s^{-1}) on the anodic oxidation current response of 0.1 mM AA has shown in Fig. 7a. As can be seen from this Figure that, as the scan rate increases the Ipa of AA has also increased simultaneously which indicates that there is a direct relationship between the oxidation peak current and the scan rate. The plot of oxidation peak current vs. square root of scan rate is shown in Fig. 7b and the results demonstrated that a diffusion-controlled reaction taken place on the modified electrode surface with a regression coefficient of $R^2 = 0.998$.

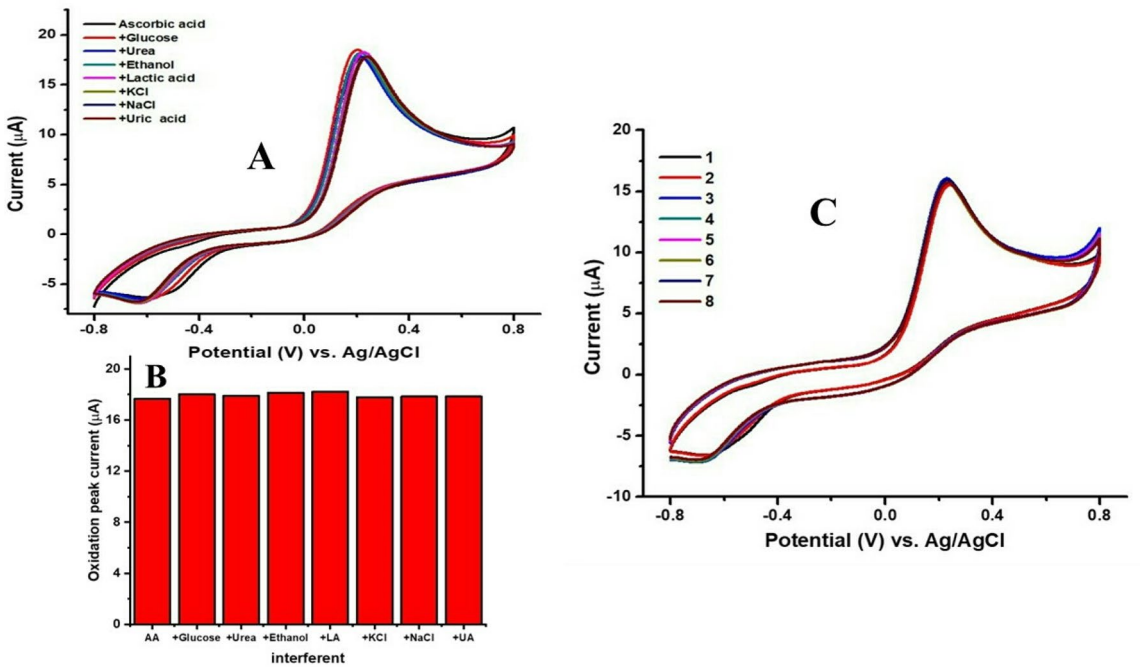

Fig. 8 **a** and **b** Effect of interfering substances/species on the Ipa response of 0.1 mM AA in 0.1 M PBS (pH 7.4) and (**c**) repeatability of the sensor

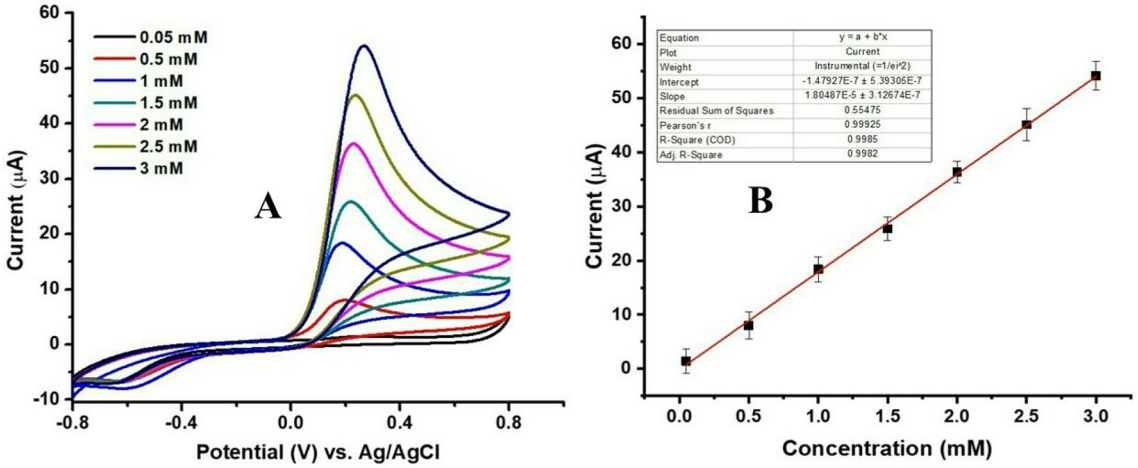

Fig. 9 **a** CV response Co_3O_4/GCE against different concentrations of AA ranging from 0.05 to 3 mM in 0.1 PBS (pH 7.4). **b** The corresponding linear plot of oxidation peak currents vs. different concentrations of AA with $R^2 = 0.998$

Selectivity, repeatability and stability

Selectivity or specificity is considered an important feature for modified electrodes. The anti-interference ability of fabricated Co_3O_4/GCE sensor was tested in 1 mM AA solution when 10 µL of each of interfering specie (of same molar concentration) such as glucose, urea, ethanol, lactic acid, KCl, NaCl and uric acid was added in the test solution. Figure 8a, b displays the selectivity results of Co_3O_4/GCE towards AA and as it can be seen from the figure that the interfering species cause a negligible effect on the oxidation peak current of AA which proves the selectivity of the proposed sensor applicable for real sample analysis. Figure 8c elucidates the repeatability results of the proposed Co_3O_4/GCE sensor in 0.1 M PBS containing 1 mM AA. For repetitive use, the sensor's response must be stable (give the same response) to many runs. To ensure this parameter, we have taken eight repeated runs on a single Co_3O_4/GCE and it exhibited excellent repeatability of the results for AA sensing which proves that the proposed sensor can be used for long-term sensing applications. Meanwhile, to make the developed sensor more reliable for long-term use, we have also investigated the stability of the Co_3O_4/GCE sensor by taking one run each day for 25 consecutive days. By doing so, no noticeable change in the Ipa response of AA was found and the sensor maintained its sensitivity of about 96.7%. But after the 25th day, the Ipa response of AA was observed to be decreased. Thus, the overall performance of the Co_3O_4/GCE sensor for 25 days was extremely good.

Analytical parameters of AA

Figure 9a represents the CV response of Co_3O_4/GCE at various concentrations of AA ranging from 0.05 to 3 mM and as it can be observed from the voltammogram that as the concentration of AA increased from 0.05 to 3 mM, the oxidation current response has also increased linearly. Figure 9b reveals the linear correlation of current response vs. various concentrations of AA with a determination coefficient of $R^2 = 0.998$. The limit of detection (LOD) and limit of quantification (LOQ) for the proposed sensor were calculated to be 0.001 mM and 0.004 mM by the given formula:

$$\text{Formula for LOD} = 3 \times {}^{SD}/_{M}, \tag{1}$$

and

$$\text{Formula for LOQ} = 10 \times {}^{SD}/_{M}, \tag{2}$$

Table 1 Comparison in the analytical performance of our fabricated Co_3O_4/GCE sensor for Qu sensing with previously reported various sensors

Modified electrode	LOD (µM)	Linear Range (µM)	References
Co3O4-CuNi/RGO/GCE	0.34	2.5–100	[56]
GO/CdTe QDs/GCE	6.1	32.3–500	[24]
HAP-ZnO–PdNPs/CPE	0.019	0.12–55.36	[3]
CuS@PB/GCE	0.24	5–3875	[57]
AgNPs/PVP/GCE	0.047	0.2–1200	[58]
Graphene flowers/CFE/GCE	73.52	45–1489	[59]
rGO-CNT/ITO	5.31	10–200	[60]
PdAu@RGO/GCE	12.5	12.5–700	[61]
Co_3O_4/GCE	1	50–3000	This work

Table 2 Determination of AA in real pharmaceutical samples using Co_3O_4/GCE sensor

Pharmaceutical samples	Mentioned amount mg/tab (mg)	Found mg/tab (mg)	RSD ($n=4$)	% Recovery
CaC 1000 + tablets	500	516.9	2.8	103
Calci sachets	500	506.3	1.79	101
Surbex Z capsules	500	530.4	2.72	106

where SD is the standard deviation of 6 runs measured in blank and *M* is the obtained slope of the calibration curve.

A comparison of our present work with previously reported studies for the electrochemical sensing of AA is given in Table 1. It can be seen from the table that the overall performance of our fabricated Co_3O_4-based GCE sensor is comparable or much better than the other reported sensors in the sense of wide detection range, low LOD, easy preparation, low-cost abilities and by just utilizing single metal oxide rather than other composite materials. Therefore, we can say that the Co_3O_4/GCE sensor could be a promising candidate for AA determination.

Analytical application

To examine the applicability of the fabricated Co_3O_4/GCE sensor in practical application, three different pharmaceutical products containing AA (vitamin C) (i) CaC 1000 +, (ii) Calci and (iii) Surbex Z were tested by calibration method [41]. The determined results are shown in Table 2. The acceptable percent recoveries and lower values of the relative standard deviation of real samples showing that the Co_3O_4/GCE sensor can be effectively used for AA detection in real samples.

Conclusion

In summary, the synthesis of IL-assisted Co_3O_4 nanostructures was carried out by a simple and facile low-temperature aqueous chemical growth procedure. The novel synthesized nanostructures were used for the modification of GCE to enhance the electrochemical performance of the electrode. The fabricated Co_3O_4/GCE sensor was used for the selective determination of AA in 0.1 M PBS of pH 7.4 and the developed sensor has shown an excellent response towards the oxidation of AA at the potential of about + 0.2 V over a concentration ranging from 0.05 to 3 mM with LOD (1 µM) and LOQ (4 µM), respectively. The proposed sensor manifested high stability, enhanced sensitivity and selectivity during chemical measurements that witnessed the practical applicability of Co_3O_4/GCE for the effective determination of AA in real samples.

Author contributions NHK: Conducting experiment and Writing of the article. IMP: Helping in characterization of material, Correction of grammatical mistakes, improving English language. JAB: Interpretation and designing of all graphs. SA: Graphing and helping in experiments. AFM: Helping in experiment and Formatting of article and references. TG: Data collection, sampling. ARS: Conceptualization/Supervision/editing/correcting draft/ Submission/Correspondence to the Journal.

References

1. Ma, X., Zhang, X., Guo, X., Kang, Q., Shen, D., Zou, G.: Sensitive and selective determining ascorbic acid and activity of alkaline phosphatase based on electrochemiluminescence of dual-stabilizers-capped CdSe quantum dots in carbon nanotube-nafion composite. Talanta **154**, 175–182 (2016)
2. Intarakamhang, S., Leson, C., Schuhmann, W., Schulte, A.: A novel automated electrochemical ascorbic acid assay in the 24-well microtiter plate format. Anal. Chim. Acta **687**(1), 1–6 (2011)
3. Shahamirifard, S.A., Ghaedi, M.: A new electrochemical sensor for simultaneous determination of arbutin and vitamin C based on hydroxyapatite-ZnO-Pd nanoparticles modified carbon paste electrode. Biosens. Bioelectron. **141**, 111474 (2019)
4. Buledi, J.A., Ameen, S., Khand, N.H., Solangi, A.R., Taqvi, I.H., Agheem, M.H., Wajdan, Z.: CuO nanostructures based electrochemical sensor for simultaneous determination of hydroquinone and ascorbic acid. Electroanalysis (2020). https://doi.org/10.1002/elan.202000083
5. Zhang, X., Cao, Y., Yu, S., Yang, F., Xi, P.: An electrochemical biosensor for ascorbic acid based on carbon-supported PdNinanoparticles. Biosens. Bioelectron. **44**, 183–190 (2013)
6. Weng, Y.-C., Lee, Y.-G., Hsiao, Y.-L., Lin, C.-Y.: A highly sensitive ascorbic acid sensor using a Ni–Pt electrode. Electrochim. Acta **56**(27), 9937–9945 (2011)
7. Choi, H.K., Gao, X., Curhan, G.: Vitamin C intake and the risk of gout in men: a prospective study. Arch. Intern. Med. **169**(5), 502–507 (2009)
8. Hu, B., Liu, Y., Wang, Z.-W., Song, Y., Wang, M., Zhang, Z., Liu, C.-S.: Bimetallic-organic framework derived porous Co3O4/Fe3O4/C-loaded g-C3N4nanocomposites as non-enzymic electrocatalysis oxidization toward ascorbic acid, dopamine acid and uric acid. Appl. Surf. Sci. **441**, 694–707 (2018)
9. Du, J., Tao, Y., Zhang, J., Xiong, Z., Xie, A., Luo, S., Li, X., Yao, C.: Co_3O_4-CuNi/reduced graphene composite for non-enzymatic detection of ascorbic acid. Mater. Technol. **34**, 1–9 (2019)
10. Jiang, J., Du, X.: Sensitive electrochemical sensors for simultaneous determination of ascorbic acid, dopamine and uric acid based on Au@ Pd-reduced graphene oxide nanocomposites. Nanoscale **6**(19), 11303–11309 (2014)
11. Grotzkyj Giorgi, M., Howland, K., Martin, C., Bonner, A.B.: A novel HPLC method for the concurrent analysis and quantitation of seven water-soluble vitamins in biological fluids (plasma and

urine): a validation study and application. Sci. World J. (2012). https://doi.org/10.1100/2012/359721
12. Wang, X., Han, Q., Cai, S., Wang, T., Qi, C., Yang, R., Wang, C.: Excellent peroxidase mimicking property of CuO/Pt nanocomposites and their application as an ascorbic acid sensor. Analyst **142**(13), 2500–2506 (2017)
13. Wang, J., Zhou, M., Dong, R., Cong, X., Zhang, R., Wang, X.: Simultaneous determination of peroxide hydrogen and ascorbic acid by capillary electrophoresis with platinum nanoparticles modified micro-disk electrode. Electroanalysis **29**(11), 2483–2490 (2017)
14. Chen, H., Wang, Q., Shen, Q., Liu, X., Li, W., Nie, Z., Yao, S.: Nitrogen doped graphene quantum dots based long-persistent chemiluminescence system for ascorbic acid imaging. Biosens. Bioelectron. **91**, 878–884 (2017)
15. Özyürek, M., Güçlü, K., Bektaşoğlu, B., Apak, R.: Spectrophotometric determination of ascorbic acid by the modified CUPRAC method with extractive separation of flavonoids–La (III) complexes. Anal. Chim. Acta **588**(1), 88–95 (2007)
16. Zhu, S., Lei, C., Gao, Y., Sun, J., Peng, H., Gao, H., Zhang, R., Wang, R., Zhao, X.-E., Wang, H.: Simple and label-free fluorescence detection of ascorbic acid in rat brain microdialysates in the presence of catecholamines. New J. Chem. **42**(5), 3851–3856 (2018)
17. Na, W., Li, N., Xingguang, S.: Enzymatic growth of single-layer MnO_2nanosheets in situ: Application to detect alkaline phosphatase and ascorbic acid in the presence of sulfanilic acid functionalized graphene quantum dots. Sens. Actuators B **274**, 172–179 (2018)
18. Peng, J., Ling, J., Zhang, X.-Q., Zhang, L.-Y., Cao, Q.-E., Ding, Z.-T.: A rapid, sensitive and selective colorimetric method for detection of ascorbic acid. Sens. Actuators B **221**, 708–716 (2015)
19. Zhang, Y., Liu, P., Xie, S., Chen, M., Zhang, M., Cai, Z., Liang, R., Zhang, Y., Cheng, F.: A novel electrochemical ascorbic acid sensor based on branch-trunk Ag hierarchical nanostructures. J. Electroanal. Chem. **818**, 250–256 (2018)
20. Abellán-Llobregat, A., Vidal, L., Rodríguez-Amaro, R., Canals, A., Morallon, E.: Evaluation of herringbone carbon nanotubes-modified electrodes for the simultaneous determination of ascorbic acid and uric acid. Electrochim. Acta **285**, 284–291 (2018)
21. Jo, A., Kang, M., Cha, A., Jang, H.S., Shim, J.H., Lee, N.-S., Kim, M.H., Lee, Y., Lee, C.: Nonenzymatic amperometric sensor for ascorbic acid based on hollow gold/ruthenium nanoshells. Anal. Chim. Acta **819**, 94–101 (2014)
22. Sha, R., Badhulika, S.: Facile green synthesis of reduced graphene oxide/tin oxide composite for highly selective and ultra-sensitive detection of ascorbic acid. J. Electroanal. Chem. **816**, 30–37 (2018)
23. Zaidi, S.A., Shahzad, F., Batool, S.: Progress in cancer biomarkers monitoring strategies using graphene modified support materials. Talanta **210**, 120669 (2020)
24. Kucukkolbasi, S., Erdogan, Z., Baslak, C., Sogut, D., Kus, M.: A highly sensitive ascorbic acid sensor based on graphene oxide/CdTe quantum dots-modified glassy carbon electrode. Russ. J. Electrochem. **55**(2), 107–114 (2019)
25. Wu, G.-H., Wu, Y.-F., Liu, X.-W., Rong, M.-C., Chen, X.-M., Chen, X.: An electrochemical ascorbic acid sensor based on palladium nanoparticles supported on graphene oxide. Anal. Chim. Acta **745**, 33–37 (2012)
26. Baksh, H., Buledi, J.A., Khand, N.H., Solangi, A.R., Mallah, A., Sherazi, S.T., Abro, M.I.: Ultra-selective determination of carbofuran by electrochemical sensor based on nickel oxide nanoparticles stabilized by ionic liquid. Monatsheftefür Chem. Chem. Mon. **151**, 1689–1696 (2020)
27. Saksena, K., Shrivastava, A., Kant, R.: Chiral analysis of ascorbic acid in bovine serum using ultrathin molecular imprinted polyaniline/graphite electrode. J. Electroanal. Chem. **795**, 103–109 (2017)
28. Wu, X., Xing, Y., Pierce, D., Zhao, J.X.: One-pot synthesis of reduced graphene oxide/metal (oxide) composites. ACS Appl. Mater. Interfaces **9**(43), 37962–37971 (2017)
29. Hussain, M.M., Asiri, A.M.: Rahman MM (2020) Non-enzymatic simultaneous detection of acetylcholine and ascorbic acid using ZnO. CuO nanoleaves: Real sample analysis. Microchem. J. **159**, 105534 (2020)
30. Bukkitgar, S.D., Kumar, S., Singh, S., Singh, V., Reddy, K.R., Sadhu, V., Bagihalli, G.B., Shetti, N.P., Reddy, C.V., Ravindranadh, K.: Functional nanostructured metal oxides and its hybrid electrodes. Recent advancements in electrochemical biosensing applications. Microchem. J. **159**, 105522 (2020)
31. Hei, Y., Li, X., Zhou, X., Liu, J., Hassan, M., Zhang, S., Yang, Y., Bo, X., Wang, H.-L., Zhou, M.: Cost-effective synthesis of three-dimensional nitrogen-doped nanostructured carbons with hierarchical architectures from the biomass of sea-tangle for the amperometric determination of ascorbic acid. Anal. Chim. Acta **1029**, 15–23 (2018)
32. Hussain, S., Zaidi, S.A., Vikraman, D., Kim, H.-S., Jung, J.: Facile preparation of tungsten carbide nanoparticles for an efficient oxalic acid sensor via imprinting. Microchem. J. **159**, 105404 (2020)
33. Ganjali, M.R., Salimi, H., Tajik, S., Beitollahi, H., Rezapour, M., Larijani, B.: Application of Fe3O4@ SiO2/MWCNT film on glassy carbon electrode for the sensitive electroanalysis of levodopa. Int. J. Electrochem. Sci. **12**(6), 5243–5253 (2017)
34. Ganjali, M.R., Beitollahi, H., Zaimbashi, R., Tajik, S., Rezapour, M., Larijani, B.: Voltammetric determination of dopamine using glassy carbon electrode modified with ZnO/Al2O3nanocomposite. Int. J. Electrochem. Sci. **13**, 2519–2529 (2018)
35. He, B.-S., Zhang, J.-X.: Rapid detection of ascorbic acid based on a dual-electrode sensor system using a powder microelectrode embedded with carboxyl multi-walled carbon nanotubes. Sensors **17**(7), 1549 (2017)
36. Shetti, N.P., Bukkitgar, S.D., Reddy, K.R., Reddy, C.V., Aminabhavi, T.M.: ZnO-based nanostructured electrodes for electrochemical sensors and biosensors in biomedical applications. Biosens. Bioelectron. **141**, 111417 (2019)
37. Dakshayini, B., Reddy, K.R., Mishra, A., Shetti, N.P., Malode, S.J., Basu, S., Naveen, S., Raghu, A.V.: Role of conducting polymer and metal oxide-based hybrids for applications in ampereometric sensors and biosensors. Microchem. J. **147**, 7–24 (2019)
38. Kumar, S., Bukkitgar, S.D., Singh, S., Singh, V., Reddy, K.R., Shetti, N.P., Venkata Reddy, C., Sadhu, V., Naveen, S.: Electrochemical sensors and biosensors based on graphene functionalized with metal oxide nanostructures for healthcare applications. ChemistrySelect **4**(18), 5322–5337 (2019)
39. Shetti, N.P., Bukkitgar, S.D., Reddy, K.R., Reddy, C.V., Aminabhavi, T.M.: Nanostructured titanium oxide hybrids-based electrochemical biosensors for healthcare applications. Colloids Surf. B **178**, 385–394 (2019)
40. Bao, L., Li, T., Chen, S., Peng, C., Li, L., Xu, Q., Chen, Y., Ou, E., Xu, W.: 3D graphene frameworks/Co3O4 composites electrode for high-performance supercapacitor and enzymeless glucose detection. Small **13**(5), 1602077 (2017)
41. Memon, S.A., Hassan, D., Buledi, J.A., Solangi, A.R., Memon, S.Q., Palabiyik, I.M.: Plant material protected cobalt oxide nanoparticles: Sensitive electro-catalyst for tramadol detection. Microchem. J. **159**, 105480 (2020)
42. Elhag, S., Ibupoto, Z., Nour, O., Willander, M.: Synthesis of Co3O4 cotton-like nanostructures for cholesterol biosensor. Materials **8**(1), 149–161 (2015)

43. Numan, A., Shahid, M.M., Omar, F.S., Ramesh, K., Ramesh, S.: Facile fabrication of cobalt oxide nanograin-decorated reduced graphene oxide composite as ultrasensitive platform for dopamine detection. Sens. Actuators B **238**, 1043–1051 (2017)
44. Song, Z., Zhang, Y., Liu, W., Zhang, S., Liu, G., Chen, H., Qiu, J.: Hydrothermal synthesis and electrochemical performance of Co3O4/reduced graphene oxide nanosheet composites for supercapacitors. Electrochim. Acta **112**, 120–126 (2013)
45. Wang, G., Zhu, F., Xia, J., Wang, L., Meng, Y., Zhang, Y.: Preparation of Co3O4/carbon derived from ionic liquid and its application in lithium-ion batteries. Electrochim. Acta **257**, 138–145 (2017)
46. Sheldon, R.: Catalytic reactions in ionic liquids. Chem. Commun. **23**, 2399–2407 (2001)
47. Fuller, J., Carlin, R.T., Osteryoung, R.A.: The room temperature ionic liquid 1-ethyl-3-methylimidazolium tetrafluoroborate: electrochemical couples and physical properties. J. Electrochem. Soc. **144**(11), 3881–3886 (1997)
48. Antonietti, M., Kuang, D., Smarsly, B., Zhou, Y.: Ionic liquids for the convenient synthesis of functional nanoparticles and other inorganic nanostructures. Angew. Chem. Int. Ed. **43**(38), 4988–4992 (2004)
49. Zheng, W., Liu, X., Yan, Z., Zhu, L.: Ionic liquid-assisted synthesis of large-scale TiO2 nanoparticles with controllable phase by hydrolysis of TiCl4. ACS Nano **3**(1), 115–122 (2008)
50. Wasserscheid, P., Welton, T.: Ionic Liquids in Synthesis. John Wiley and Sons, Amsterdam (2008)
51. Shen, J., Shi, M., Yan, B., Ma, H., Li, N., Ye, M.: Ionic liquid-assisted one-step hydrothermal synthesis of TiO 2-reduced graphene oxide composites. Nano Res. **4**(8), 795 (2011)
52. Al-Qirby, L.M., Radiman, S., Siong, C.W., Ali, A.M.: Sonochemical synthesis and characterization of Co_3O_4 nanocrystals in the presence of the ionic liquid [EMIM][BF4]. Ultrason. Sonochem. **38**, 640–651 (2017)
53. Chang, A.S., Memon, N.N., Amin, S., Chang, F., Aftab, U., Abro, M.I., dad Chandio, A., Shah, A.A., Ibupoto, M.H., Ansari, M.A.: Facile non-enzymatic lactic acid sensor based on cobalt oxide nanostructures. Electroanalysis **31**(7), 1296–1303 (2019)
54. Vinothkumar, V., Sangili, A., Chen, S.M., Veerakumar, P., Lin, K.-C.: Sr-doped NiO3 nanorods synthesized by simple sonochemical method as excellent materials for voltammetric determination of quercetin. New J. Chem. **44**, 2821–2832 (2020)
55. Zhao, P., Ni, M., Xu, Y., Wang, C., Chen, C., Zhang, X., Li, C., Xie, Y., Fei, J.: A novel ultrasensitive electrochemical quercetin sensor based on MoS2-carbon nanotube@ graphene oxide nanoribbons/HS-cyclodextrin/graphene quantum dots composite film. Sens. Actuators B **299**, 126997 (2019)
56. Du, J., Tao, Y., Zhang, J., Xiong, Z., Xie, A., Luo, S., Li, X., Yao, C.: Co3O4-CuNi/reduced graphene composite for non-enzymatic detection of ascorbic acid. Mater. Technol. **34**(11), 665–673 (2019)
57. Li, L., Zhang, P., Li, Z., Li, D., Han, B., Tu, L., Li, B., Wang, Y., Ren, L., Yang, P.: CuS/Prussian blue core–shell nanohybrid as an electrochemical sensor for ascorbic acid detection. Nanotechnology **30**(32), 325501 (2019)
58. Karaboduk, K.: Electrochemical determination of ascorbic acid based on AgNPs/PVP-modified glassy carbon electrode. ChemistrySelect **4**(20), 6361–6369 (2019)
59. Du, J., Yue, R., Ren, F., Yao, Z., Jiang, F., Yang, P., Du, Y.: Novel graphene flowers modified carbon fibers for simultaneous determination of ascorbic acid, dopamine and uric acid. Biosens. Bioelectron. **53**, 220–224 (2014)
60. Zhang, Y., Ji, Y., Wang, Z., Liu, S., Zhang, T.: Electrodeposition synthesis of reduced graphene oxide–carbon nanotube hybrids on indium tin oxide electrode for simultaneous electrochemical detection of ascorbic acid, dopamine and uric acid. RSC Adv. **5**(129), 106307–106314 (2015)
61. Zou, C.E., Zhong, J., Li, S., Wang, H., Wang, J., Yan, B., Du, Y.: Fabrication of reduced graphene oxide-bimetallic PdAunanocomposites for the electrochemical determination of ascorbic acid, dopamine, uric acid and rutin. J. Electroanal. Chem. **805**, 110–119 (2017)